Chinese Journal of Chemical Engineering 70 (2024) 211–221

Contents lists available at ScienceDirect

Chinese Journal of Chemical Engineering

journal homepage: www.elsevier.com/locate/CJChE

Full Length Article

Complete kinetic model for esterification reaction of lauric acid with glycerol to synthesize glycerol monolaurate

Han-Qiao Hu [1], Yue Zhang [1], Ming Fan [3], Yong Cai [3], Guang-Wen Chu [1, 2], Liang-Liang Zhang [1, 2, *]

[1] *Research Center of the Ministry of Education for High Gravity Engineering and Technology, Beijing University of Chemical Technology, Beijing 100029, China*
[2] *State Key Laboratory of Organic-Inorganic Composites, Beijing University of Chemical Technology, Beijing 100029, China*
[3] *Petrochemical Research Institute, China National Petroleum Corporation, Beijing 102206, China*

ARTICLE INFO

Article history:
Received 24 November 2023
Received in revised form
18 March 2024
Accepted 18 March 2024
Available online 12 April 2024

Keywords:
Glycerol monolaurate
p-Toluenesulfonic acid
Esterification
Kinetics
Mass transfer

ABSTRACT

Glycerol monolaurate (GML) is a widely used industrial chemical with excellent emulsification and antibacterial effect. The direct esterification of glycerol with lauric acid is the main method to synthesize GML. In this work, the kinetic process of direct esterification was systematically studied using *p*-toluenesulfonic acid as catalyst. A complete kinetic model of consecutive esterification reaction has been established, and the kinetic equation of acid catalysis was deduced. The isomerization reactions of GML and glycerol dilaurate were investigated. It was found that the reaction was an equilibrium reaction and the reaction rate was faster than the esterification reaction. The kinetic equations of the consecutive esterification reaction were obtained by experiments as $k_1 = (276+92261X_{cat})\exp(-37720/RT)$ and $k_2 = (80+4413X_{cat})\exp(-32240/RT)$. The kinetic results are beneficial to the optimization of operating conditions and reactor design in GML production process.

1. Introduction

Glycerol monolaurate (GML) is a medium-chain fatty acid glyceride, which is naturally present in breast milk, coconut oil and palm oil [1]. It is a stable non-ionic surfactant with excellent emulsification effect [2]. In addition, GML is a safe, efficient and broad-spectrum antibacterial agent, which has a good inhibitory effect on bacteria, fungi and viruses [3]. The US Food and Drug Administration had recognized GML as a safe food additive since 1977 [4]. Hence, GML is widely used in food, cosmetics and pharmaceutical [5–7].

At present, the synthesis methods of GML mainly include direct esterification of glycerol (GL) and lauric acid (LA), glycerolysis of triglycerides and glycerolysis of methyl laurate [8–10]. Among them, the direct esterification method has been widely used to prepare GML due to its simple process, which obtains GML by direct esterification of GL and LA under the condition of acid catalyst [11].

The direct esterification reaction of LA and GL reported in the literatures is a consecutive reaction process including monoesterification reaction (R1), diesterification reaction (R2) and triesterification reaction (R3) [12–14]. Glycerol dilaurate (GDL) has 1,3-GDL and 1,2-GDL two isomers, and these isomers can reach equilibrium by isomerization reaction [15]. Similarly, GML has α-GML and β-GML two isomers [16], so these isomers will also undergo isomerization reaction. As a result, the reaction network of direct esterification of GL and LA can be concluded as Fig. 1.

The kinetic result is one of the significant factors for reactor design and process control. Some scholars have studied the esterification kinetics of GL and LA. Oktavianty *et al.* [17] studied the kinetics of R1 under dealuminated zeolite Y catalyst. The first and second order reaction kinetic model were tested, and the experimental results show that the R1 is a second order reaction. Han *et al.* [18] used ionic liquid–silicotungstic acid composites as catalyst, established second order reaction kinetic model of R1 and obtained the same conclusion. Shen *et al.* [19] used the second order reaction kinetics model to study the reaction kinetics of R1 under boric acid based deep eutectic solvent. They obtained kinetic constant such as reaction rate constant and activation energy through experiments, and the experimental data with model fit

* Corresponding author. Tel.: +86 10 64443134; Fax: +86 10 64434784.
E-mail address: zhll@mail.buct.edu.cn (L.-L. Zhang).

https://doi.org/10.1016/j.cjche.2024.03.013

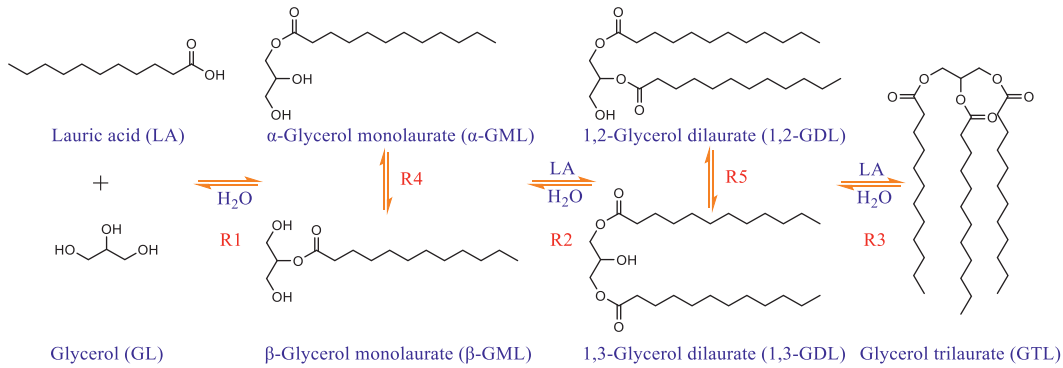

Fig. 1. The esterification reaction process of glycerol and lauric acid.

well. For the synthesis of GML, these authors only studied the main reaction R1 but not the side reaction R2, so their kinetic studies are not comprehensive enough.

Szelag *et al.* [20] and Macierzanka *et al.* [21] studied the kinetics of consecutive esterification of LA and GL in the presence of different carboxylate. Under the condition of continuous distillation, they regarded the esterification reaction as an irreversible reaction. Then, they established first order consecutive reaction kinetic models of R1, R2, and R3, and the reaction rate constant and activation energy of the main reaction R1 and the side reaction R2 were obtained by experiments. Han *et al.* [22] studied the kinetics of consecutive esterification reaction under silica gel-based sulfonic acid functionalized ionic liquid catalysts. Under the experimental conditions of excessive GL, they regarded the esterification reaction as an irreversible first order reaction, and established reaction kinetic models. The kinetic results of these literatures are not comprehensive enough. More investigation should be done to instruct reactor design. Firstly, the mass transfer process should be considered in the synthesis with a heterogeneous system to make kinetic results more intrinsic. Secondly, the reaction network and kinetic model should include the isomerization reactions and the analytical method should be improved to track all reactions.

In this work, the kinetics of direct esterification of LA and GL was systematically studied by experiments using *p*-toluenesulfonic acid as catalyst. A complete kinetic model of consecutive esterification reaction was established, which considered the isomerization reactions of GML and GDL. The isomerization reactions of GML and GDL were investigated. Under the condition of eliminating the influence of reversible reaction and mass transfer, the reaction kinetics parameters such as reaction orders of reactants and catalyst, reaction rate constant, activation energy and pre-exponential factor were determined. Based on the kinetic results, the influence of mass transfer process on esterification was discussed.

2. Experimental and Kinetic Modelling

2.1. Materials

Lauric acid (≥98%), glycerol (≥99.5%), trimethylchlorosilane (≥98%), *p*-toluenesulfonic acid (≥99%) and pyridine (AR) were purchased from Shanghai Macklin Biochemical Technology Co., Ltd. Myristic acid (≥99%), hexamethyl disilylamine (≥98%) and 1,3-dilaurin glycerol (≥96%) were purchased from Shanghai Aladdin Biochemical Technology Co., Ltd. α-Monolaurin (≥98%) were purchased from Shanghai Yuanye Biochemical Technology Co., Ltd. N_2 were purchased from Beijing Shunanqite Gas Co., Ltd.

2.2. Experiment and procedure

The esterification reaction of GL and LA was carried out in a 50 ml four-necked flask. The stirring process was controlled by a magnetic stirrer and the stirrer was an olive type with a size of 25 mm. The reaction temperature was controlled by an oil bath and measured by a temperature detector. The concentration of the reaction mixture was monitored by gas chromatography (GC). In the experimental process, N_2 was used to maintain an inert environment and remove water, and its flow rate was controlled by a flow mass controller (see Fig. 2).

Firstly, the reactant LA of 40 g was added to the flask, the nitrogen valve was opened and the flow rate was controled to 0.1 $L \cdot min^{-1}$ after the LA melted. Secondly, the catalyst *p*-toluenesulfonic acid was added to GL to prepare a GL solution with a

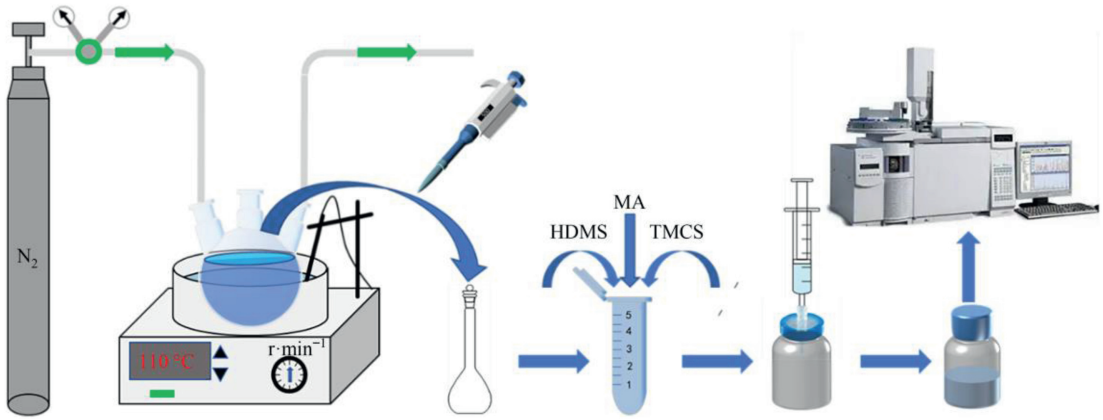

Fig. 2. The schematic diagram of the kinetics experimental setup.

certain mole fraction, then it was heated. Finally, when the reactants GL and LA were heated to the desired temperature, a certain volume of GL was added to the flask, then the reaction started. The kinetic experiments were performed using the mole ratio of LA with GL as 34:1, the rotating speed as 700 r·min^{-1}, the temperatures of 383–423 K, and the molar content of catalyst of 0.5% to 2.0%. The sample of 0.5 ml was taken from the flask with a pipette to volumetric flask at regular intervals. The sample was rapidly cooled down with ice water to stop the reaction, then pyridine was added to dissolve sample. The sampling time of the first sample was regarded as the zero point of reaction time. The concentration of first sample was regarded as the initial concentration. In this way. the influence of mixing on the reaction can be eliminated.

2.3. Analytical method

The concentration of each substance was determined by GC with internal standardization, and the internal standard was a solution of myristic acid with a concentration of 50 mg·ml^{-1}. Due to the high boiling point of each substance in the system, the reaction mixture needed to be silanized. The silane reagent was hexamethyl disilylamine, and trimethylchlorosilane was used as catalyst. The sample solution, myristic acid, trimethylchlorosilane and hexamethyl disilylamine were mixed with a volume ratio of 2:1:2:4. The mixed solution was put into a 50 °C oven for silylation for 5 h.

The determinations of reaction products concentrations were carried out using gas chromatography (GC-2014C Shimadzu Research Laboratory Co. Ltd) equipped with a dimethylpolysiloxane chromatographic column (DB-1HT, 15 m×0.25 mm×0.10 μm). The temperature was programmed as follows: The GC column initial temperature was 120 °C, and increased thereafter to 240 °C at a rate of 10 °C·min^{-1}, then raised at 15 °C·min^{-1} to 300 °C, and maintained at that temperature 3 min.

2.4. Kinetic model

We assume that all esterification reactions are irreversible pseudo-first-order reactions under certain conditions as Refs. [20–22]. This assumption can be achieved by using excessive LA and removing water in the experiment. Under this assumption, the reaction network of GL and LA can be simplified as shown in Fig. 3. According to the reaction network, the reaction rate of GL, GML and GDL can be described as follows:

$$-\frac{dC_{GL}}{dt} = k_{11}C_{LA}C_{GL} + k_{12}C_{LA}C_{GL} = (k_{11}+k_{12})C_{LA}C_{GL} = k_1C_{LA}C_{GL} \tag{1}$$

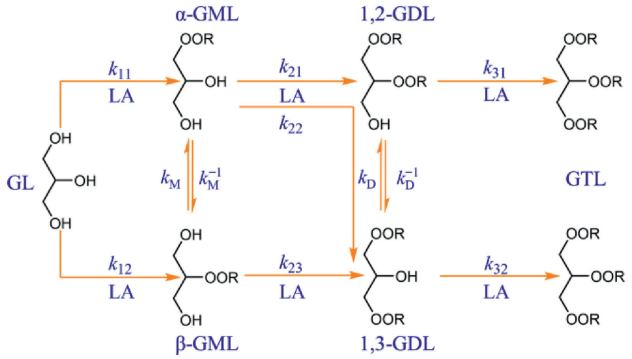

Fig. 3. The simplified reaction kinetics network of glycerol and lauric acid.

$$\frac{dC_{GML}}{dt} = k_1C_{LA}C_{GL} - (k_{21}+k_{22})C_{LA}C_{\alpha-GML} - k_{23}C_{LA}C_{\beta-GML} \tag{2}$$

$$\frac{dC_{GDL}}{dt} = (k_{21}+k_{22})C_{LA}C_{\alpha-GML} + k_{23}C_{LA}C_{\beta-GML} - k_{31}C_{LA}C_{1,2-GDL} - k_{32}C_{LA}C_{1,3-GDL} \tag{3}$$

where, k_{11}, k_{12} and k_1 are the reaction rate constants of LA reacting with GL to produce α-GML, β-GML and total GML, respectively. The variables k_{21} and k_{22} are the reaction rate constants of LA reacting with α-GML to produce 1,2-GDL and 1,3-GDL, respectively. The variables k_{23} is the reaction rate constant of LA reacting with β-GML to form 1,3-GDL. The variables k_{31} and k_{32} are the reaction rate constants of LA reacting with 1,2-GDL and 1,3-GDL to form GTL, respectively.

It is assumed that the isomerization reactions of GML and GDL can quickly reach equilibrium, then the following equations can be deduced:

$$\eta_M = \frac{C_{\alpha-GML}}{C_{GML}} = \frac{k_M}{k_M + k_M^{-1}} \tag{4}$$

$$\eta_D = \frac{C_{1,3-GDL}}{C_{GDL}} = \frac{k_D^{-1}}{k_D + k_D^{-1}} \tag{5}$$

where, η_M is the ratio of α-GML to total GML; η_D is the ratio of 1,3-GDL to total GDL; k_M and k_M^{-1} are positive reaction rate constants and reverse reaction rate constants of GML isomer conversion reaction, respectively; k_D and k_D^{-1} are positive reaction rate constants and reverse reaction rate constants of GDL isomer conversion reaction, respectively.

According to the isomerization reaction assumption, η_M and η_D are always a constant, which will be proved in later experiments. Combining Eq. (4) and Eq. (5) with Eq. (2) and Eq. (3) respectively, then Eq. (2) and Eq. (3) can be described as follows:

$$\begin{aligned}\frac{dC_{GML}}{dt} &= k_1C_{LA}C_{GL} - (\eta_M(k_{21}+k_{22}) + (1-\eta_M)k_{23})C_{LA}C_{GML} \\ &= k_1C_{LA}C_{GL} - k_2C_{LA}C_{GML}\end{aligned} \tag{6}$$

$$\begin{aligned}\frac{dC_{GDL}}{dt} &= k_2C_{LA}C_{GML} - (\eta_Dk_{31} + (1-\eta_D)k_{32})C_{LA}C_{GDL} \\ &= k_2C_{LA}C_{GML} - k_3C_{LA}C_{GDL}\end{aligned} \tag{7}$$

where, k_2 is the reaction rate constants of LA reacting with total GML to produce total GDL; k_3 is the reaction rate constants of LA reacting with total GDL to produce GTL.

Under the condition of excessive LA, the concentration of LA is approximately unchanged. Hence, Eq. (1), Eq. (6) and Eq. (7) can be described as follows:

$$-\frac{dC_{GL}}{dt} = k_1'C_{GL} \tag{8}$$

$$\frac{dC_{GML}}{dt} = k_1'C_{GL} - k_2'C_{GML} \tag{9}$$

$$\frac{dC_{GDL}}{dt} = k_2'C_{GML} - k_3'C_{GDL} \tag{10}$$

where, k'_1, k'_2 and k'_3 are the product of LA concentration and k_1, k_2, k_3, respectively.

Use the matrix to solve the above differential equations to obtain the general solution, and then obtain the special solution according to the initial concentration condition. Finally, the relationship between substance concentration and time can be written as follows.

$$\frac{C_{GL}}{C_{GL_0}} = e^{-k'_1 t} \tag{11}$$

$$\frac{C_{GML}}{C_{GL_0}} = \frac{k'_1}{k'_1 - k'_2}\left(e^{-k'_2 t} - e^{-k'_1 t}\right) + \frac{C_{GML_0}}{C_{GL_0}} e^{-k'_2 t} \tag{12}$$

$$\begin{aligned}\frac{C_{GDL}}{C_{GL_0}} = &\frac{k'_1 k'_2}{k'_1 - k'_2}\left(\frac{e^{-k'_2 t} - e^{-k'_3 t}}{k'_3 - k'_2} - \frac{e^{-k'_1 t} - e^{-k'_3 t}}{k'_3 - k'_1}\right) + \\ &\frac{C_{GML_0}}{C_{GL_0}}\frac{k'_2}{k'_3 - k'_2}\left(e^{-k'_2 t} - e^{-k'_3 t}\right) + \frac{C_{GDL_0}}{C_{GL_0}} e^{-k'_3 t}\end{aligned} \tag{13}$$

The experiment can obtain the concentration of each substance at different times, then the reaction rate constant can be obtained by non-linear fitting according to Eqs. (11)–(13). For the synthesis of GML, only the reaction rate constants of main reaction R1 and side reaction R2 is the key kinetic parameters.

P-toluenesulfonic acid is an organic homogeneous acidic catalyst with good catalytic effect and no oxidation, which is widely used in direct esterification [23]. Therefore, *p*-toluenesulfonic acid is selected as the direct esterification catalyst. The main feature of acid catalysis is proton transfer. The process of acid catalysis generally includes two steps. Firstly, reactant LA combines with proton to form proton compound. Secondly, proton compounds react with reactants GL or GML or GDL to produce products and release protons. The acid catalyzed esterification reaction process can be written as follows:

$$A + H^+ \rightleftharpoons AH^+ \tag{14}$$

$$AH^+ + B \rightarrow AB + H^+ + H_2O \tag{15}$$

where, A is LA, AH^+ is intermediate product, B is GL or GML or GDL, AB represents products GML or GDL or GTL.

The first step is a fast equilibrium reaction, which can be described by Eq. (16). The second step is a slow nucleophilic substitution reaction, which is the rate controlling step. So, the total reaction rate can be expressed by Eq. (17).

$$k_A C_A C_{H^+} = k_{-A} C_{AH^+} \tag{16}$$

$$\frac{dC_{AB}}{dt} = k_{AB} C_{AH^+} C_B \tag{17}$$

Eq. (18) is obtained by substituting Eq. (16) into Eq. (17). Then, the apparent reaction rate constant can be expressed by Eq. (19):

$$\frac{dC_{AB}}{dt} = k_{AB}\frac{k_A}{k_{-A}} C_{H^+} C_A C_B = k C_A C_B \tag{18}$$

$$k = k_0 \exp\left(\frac{E}{RT}\right) C_{H^+} \tag{19}$$

where, k is the apparent reaction rate constant, k_0 is the apparent preexponential factor, E is the apparent activation energy.

According to the catalytic process, the catalytic effect mainly comes from hydrogen proton. The concentration of hydrogen proton can be expressed by the following Eq. (20) [24].

$$C_{H^+} = a + p C_{cat}^q \tag{20}$$

where, C_{cat} is catalyst concentration, a and p are constants, a is the proton contributed by the self-decomposition of LA, p is the catalyst action coefficient, q is the power of C_{cat}.

The catalyst *p*-toluenesulfonic acid used in this experiment is a homogeneous strong acid, the catalyst concentration is theoretically proportional to the proton concentration provided. Hence, the value of q should equal to 1. The catalyst dosage used in this experiment is expressed in X_{cat}, X_{cat} is molar content of catalyst in reactant GL. Because the accurate value of reaction volume is difficult to obtain, X_{cat} is used instead of C_{cat}. X_{cat} is proportional to C_{cat}, so the influence of temperature and catalyst dosage on the reaction rate constant can be described by following equation.

$$k = k_0 \exp\left(\frac{E}{RT}\right)(a + bX_{cat}) \tag{21}$$

where, b is the catalyst action coefficient.

3. Results and Discussion

3.1. Verification of assumptions of kinetics model

3.1.1. Verification of irreversible reaction assumption

In order to eliminate the influence of reversible reaction and achieve the irreversible first order reaction assumption proposed in the kinetic model, excessive LA was used in the experiment. Therefore, the molar ratio of lauric acid to glycerol is very high, the forward reaction rate of esterification reaction is far greater than the reverse reaction rate, which can reduce the effect of reversible reaction [22,25,26]. N_2 introduced in the experiment can remove some water, which can also reduce the reversible reaction rate [27]. Under the action of the above two factors, the influence of reversible reaction can be eliminated. In addition, GL is not much soluble in LA, and the solubility is only 23.0% mass at 180 °C [28]. When lauric acid is excessive, the esterification reaction is a homogeneous reaction process, which can eliminate the influence of mixing and make kinetic results are more intrinsic.

When the molar ratio is too large, the GL concentration will be small, then the detection error of GC will increase. In order to find the suitable molar ratio, the effect of molar ratio of LA to GL on the reaction was investigated experimentally. The results are shown in following Fig. 4. According to Eq. (11)–(13), the changes of C_{GL}/C_{GL0}, C_{GML}/C_{GL0} and C_{GDL}/C_{GL0} with time are closely related to the reaction rate constant (k'_1, k'_2 and k'_3). The volume of LA is much larger than that of GL under experimental conditions, so the concentration of LA is basically unchanged, then the value of k' is only related to k. When the condition of excessive LA cannot be reached, reversible reaction will reduce the reaction rate.

Fig. 4(a)–(c) show the changes of C_{GL}/C_{GL0}, C_{GML}/C_{GL0} and C_{GDL}/C_{GL0} with time. It is seen that when the molar ratio is lower than 34, the consumed rate of GL and the generation rate of GML and GDL increase with the increase of molar ratio; when the molar ratio is above 34, the changes of C_{GL}/C_{GL0}, C_{GML}/C_{GL0} and C_{GDL}/C_{GL0} with time basically coincides. Therefore, the molar ratio of LA to GL is selected 34 in subsequent experiment, which reaches the experimental condition of excessive LA.

3.1.2. Verification of isomerization reaction assumption

To verify the assumption that the reaction between GML or GDL isomers is faster than the esterification reaction proposed in the kinetic reaction model. The reaction of LA with α-GML and the reaction of LA with 1,3-GDL were investigated respectively by experiments under the experimental conditions of excessive lauric acid. The experimental results are as shown in Fig. 5.

For the reaction of LA with α-GML, when conversion reaction of α-GML and β-GML can quickly reach balance, Eq. (22), Eq. (23) and Eq. (24) can be obtained according to the reaction kinetics network and Eq. (6):

$$-\frac{dC_{\alpha-GML}}{dt} = (k'_{21} + k'_{22})C_{\alpha-GML} \quad (22)$$

$$-\frac{dC_{\beta-GML}}{dt} = k'_{23}C_{\beta-GML} \quad (23)$$

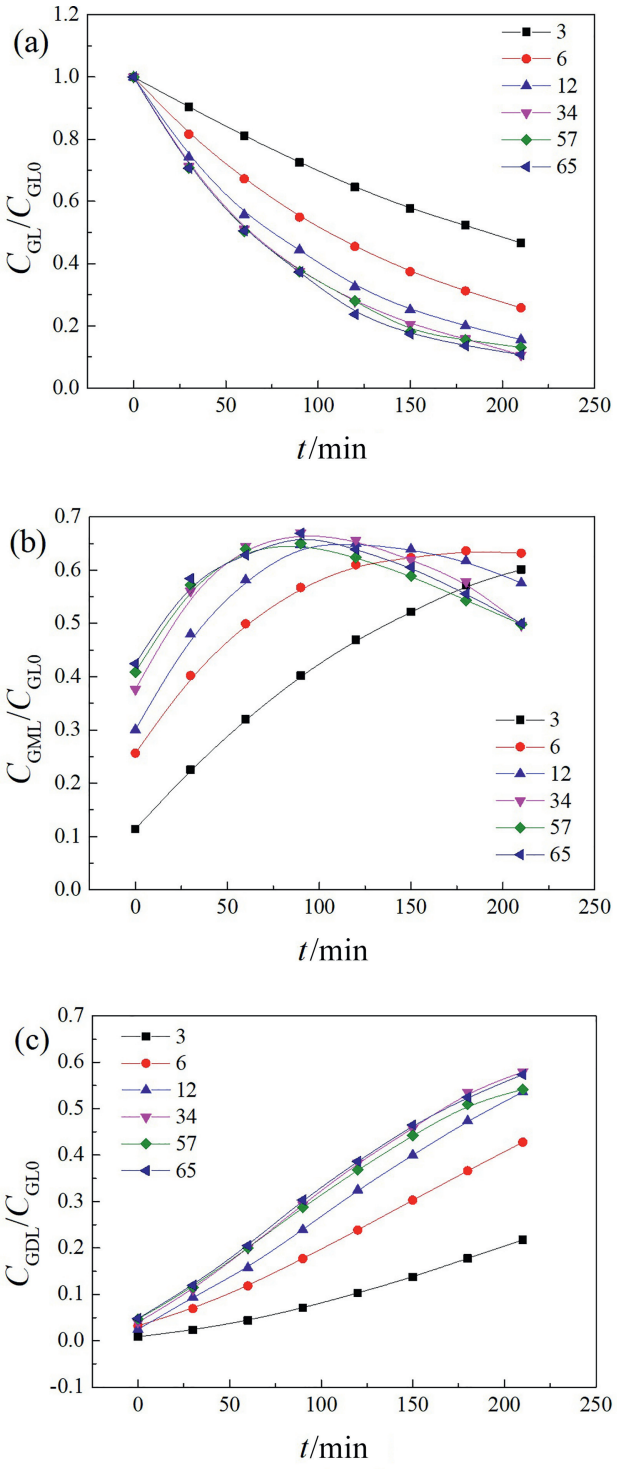

Fig. 4. Effect of different molar ratio of LA to GL (3, 6, 12, 34, 57, 65) on (a) C_{GL}/C_{GL0}, (b) C_{GML}/C_{GL0}, (c) C_{GDL}/C_{GL0} at 403.15 K and 1000 r·min^{-1}.

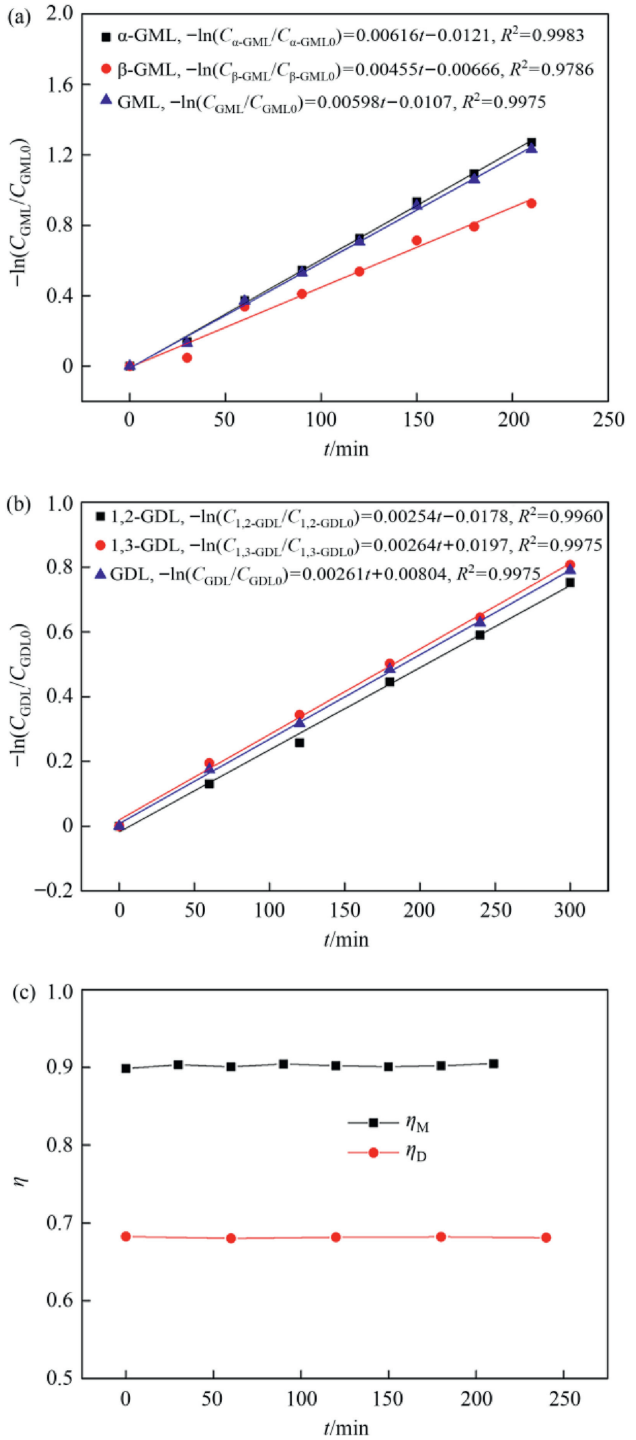

Fig. 5. Plot of (a) $-\ln(C_{GML}/C_{GML0})$, (b) $-\ln(C_{GDL}/C_{GDL0})$, (c) η *versus* t at 403.15 K.

$$-\frac{dC_{GML}}{dt} = k'_2 C_{GML} \tag{24}$$

$$\eta_M(k'_{21} + k'_{22}) + (1 - \eta_M)k'_{23} = k'_2 \tag{25}$$

where, k'_{21}, k'_{22} and k'_{23} are the product of LA concentration and k_{21}, k_{22}, k_{23}, respectively.

Eqs. (26)–(28) are obtained by solving Eqs. (22)–(24). The value of k'_{21} plus k'_{22}, k'_{23} and k'_2 can be obtained by linear fitting according to Eqs. (26)–(28), when conversion reaction of α-GML and β-GML can quickly reach equilibrium, these reaction rate constants will satisfy Eq. (25).

$$-\ln\frac{C_{\alpha-GML}}{C_{\alpha-GML0}} = (k'_{21} + k'_{22})t \tag{26}$$

$$-\ln\frac{C_{\beta-GML}}{C_{\beta-GML0}} = k'_{23}t \tag{27}$$

$$-\ln\frac{C_{GML}}{C_{GML0}} = k'_2 t \tag{28}$$

similarly, for the reaction of LA with 1,3-GML, there are the following equations:

$$-\frac{dC_{1,2-GDL}}{dt} = k'_{31} C_{1,2-GDL} \tag{29}$$

$$-\frac{dC_{1,3-GDL}}{dt} = k'_{32} C_{1,3-GDL} \tag{30}$$

$$-\frac{dC_{GDL}}{dt} = k'_3 C_{GDL} \tag{31}$$

$$\eta_D k'_{31} + (1 - \eta_D)k'_{32} = k'_3 \tag{32}$$

where, k'_{31} and k'_{32} are the product of LA concentration and k_{31}, k_{32} respectively.

Eqs. (33)–(35) are obtained by solving Eqs. (29)–(31). The value of k'_{31}, k'_{32} and k'_3 can be obtained by linear fitting according to Eqs. (33)–(35). When conversion reaction of 1,2-GDL and 1,3-GDL can quickly reach equilibrium, these reaction rate constants will satisfy Eq. (32).

$$-\ln\frac{C_{1,2-GDL}}{C_{1,2-GDL0}} = k'_{31}t \tag{33}$$

$$-\ln\frac{C_{1,3-GDL}}{C_{1,3-GDL0}} = k'_{32}t \tag{34}$$

$$-\ln\frac{C_{GDL}}{C_{GDL0}} = k'_3 t \tag{35}$$

Fig. 5(a) and (b) show the linear regression of plot of $-\ln(C_{GML}/C_{GML0})$ and $-\ln(C_{GDL}/C_{GDL0})$ *versus* time, respectively. For the reaction of α-GML with LA, the detection of β-GML in the product indicates that α-GML and β-GML can be transformed into each other. Similarly, 1,3-GDL and 1,2-GDL can be transformed into each other. The fitting results have a good linear relationship, which indicates that the esterification reaction conforms to the first order reaction law, the results are consistent with previous assumptions. The fitting results of reaction rate constant are in good consistence with Eqs. (25) and (32), which proves the isomerization reaction assumption. Fig. 5(c) shows the relationship of η_M and η_D with time. It is seen that η_M and η_D don't change with time basically, the value of η_M and η_D are 0.9 and 0.68 respectively, which conforms to Eqs. (4) and (5). It also proves that the conversion reaction between the isomers is an equilibrium reaction and is faster than the esterification reaction.

3.2. Study of reaction kinetic characteristics

3.2.1. Elimination of mass transfer effect

In order to eliminate the influence of mass transfer process on the reaction and make the kinetic results more intrinsic. The effect of different rotational speed on esterification reaction was investigated by experiments. The results are presented in Fig. 6.

Fig. 6(a)–(c) shows that when the rotating speed is above 700 $r \cdot min^{-1}$, the changes of C_{GL}/C_{GL0}, C_{GML}/C_{GL0} and C_{GDL}/C_{GL0} with time basically coincides, which indicates that the reaction rate constants are stable. Therefore, the rotating speed is selected as 700 $r \cdot min^{-1}$, the effect of mass transfer is thought to be eliminated.

3.2.2. Effect of temperature on kinetics

To obtain various parameters in Eq. (21), the effect of temperature on the reaction rate is investigated by experiments. The results are displayed in Fig. 7.

Fig. 7(a) and (b) show the non-linear fitting results of C_{GL}/C_{GL0} and C_{GML}/C_{GL0} with time, respectively. It can be seen from the figure that the correlation coefficients of each line are basically above 0.99, which indicates the experimental data is in good consistence with Eqs. (11) and (12). It is proved that the kinetic mathematical model is correct. Fig. 7(c) presents the linear regression of plot of $\ln k_1$ and $\ln k_2$ *versus* $1000/T$, and the fitting results have good linearity, which conforms to Eq. (36).

$$\ln k = \ln(k_0(a + bX_{cat})) - \frac{E}{RT} \tag{36}$$

The reaction rate constant k_1 and k_2 of different temperatures can be obtained according to the fitting results in Fig. 7(a) and (b), respectively. The activation energy E_1 and E_2 can be deduced based on results of Fig. 7(c). The values of kinetic rate constant at different temperatures and activation energy are displayed in Table 1.

3.2.3. Effect of catalyst dosages on kinetics

In order to further obtain the parameters in Eq. (21) and verify the acidic catalytic process, the effect of catalyst dosage on the reaction rate is explored. The results are displayed in Fig. 8.

Fig. 8(a) and (b) show the non-linear fitting results of C_G/C_{G0} and C_M/C_{G0} with time, respectively. It can be seen from the figure that the correlation coefficients are above 0.99, which demonstrates that the mathematical model is correct. Fig. 8(c) presents the linear regression of plot of k_1 and k_2 *versus* X_{cat}, and the data is in good consistence with Eq. (25), which proves the correctness of acid catalysis process.

$$k = bk_0 \exp\left(\frac{E}{RT}\right)X_{cat} + ak_0 \exp\left(\frac{E}{RT}\right) \tag{37}$$

The reaction rate constant k_1 and k_2 of different catalyst dosages can be obtained according to the fitting results in Fig. 8(a) and (b), respectively. The activation energy has been calculated previously, so the ak_{10}, bk_{10}, ak_{20} and bk_{20} can be deduced based on results of Fig. 8(c). The values are displayed in Table 2.

Relevant reaction parameters can be obtained through the experimental exploration of the amount of catalyst and temperature on the reaction rate. The following reaction rate equation can be obtained by substituting the relevant parameters into Eq. (21).

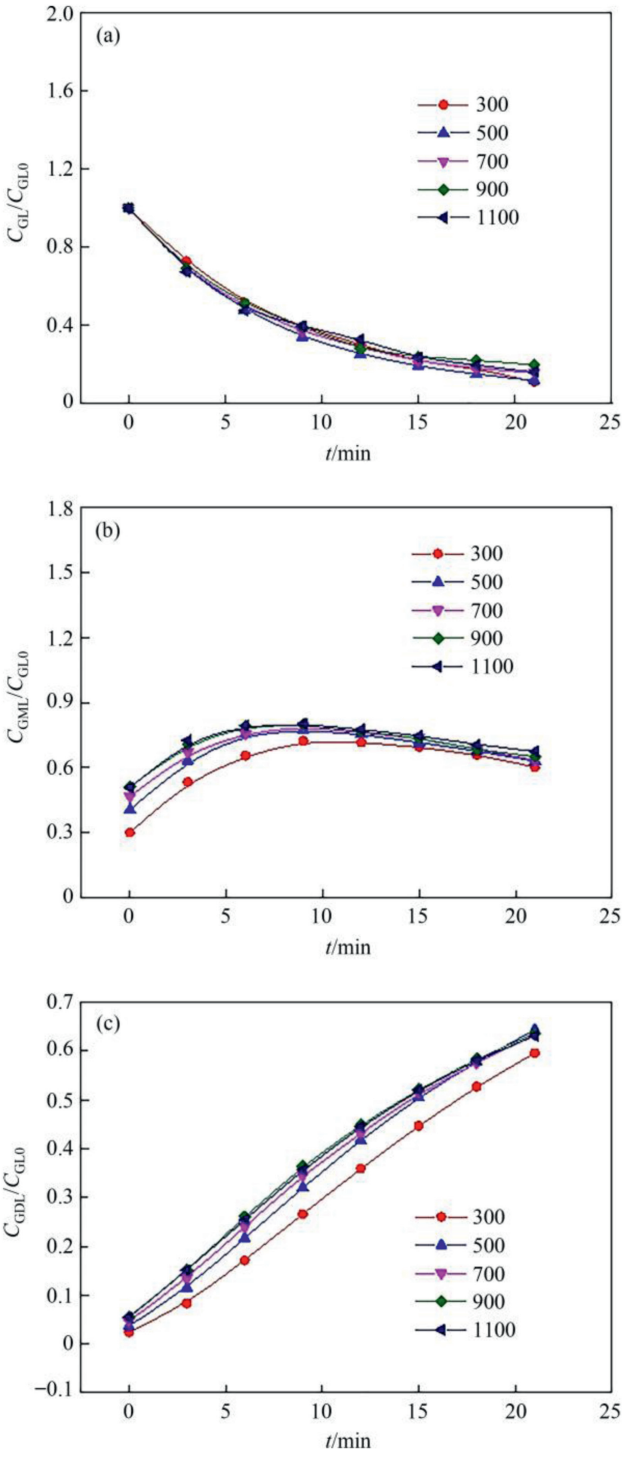

Fig. 6. Effect of rotating speed on (a) C_{GL}/C_{GL0}, (b) C_{GML}/C_{GL0}, (c) C_{GDL}/C_{GL0} at 403.15 K and 2% *p*-toluenesulfonic acid.

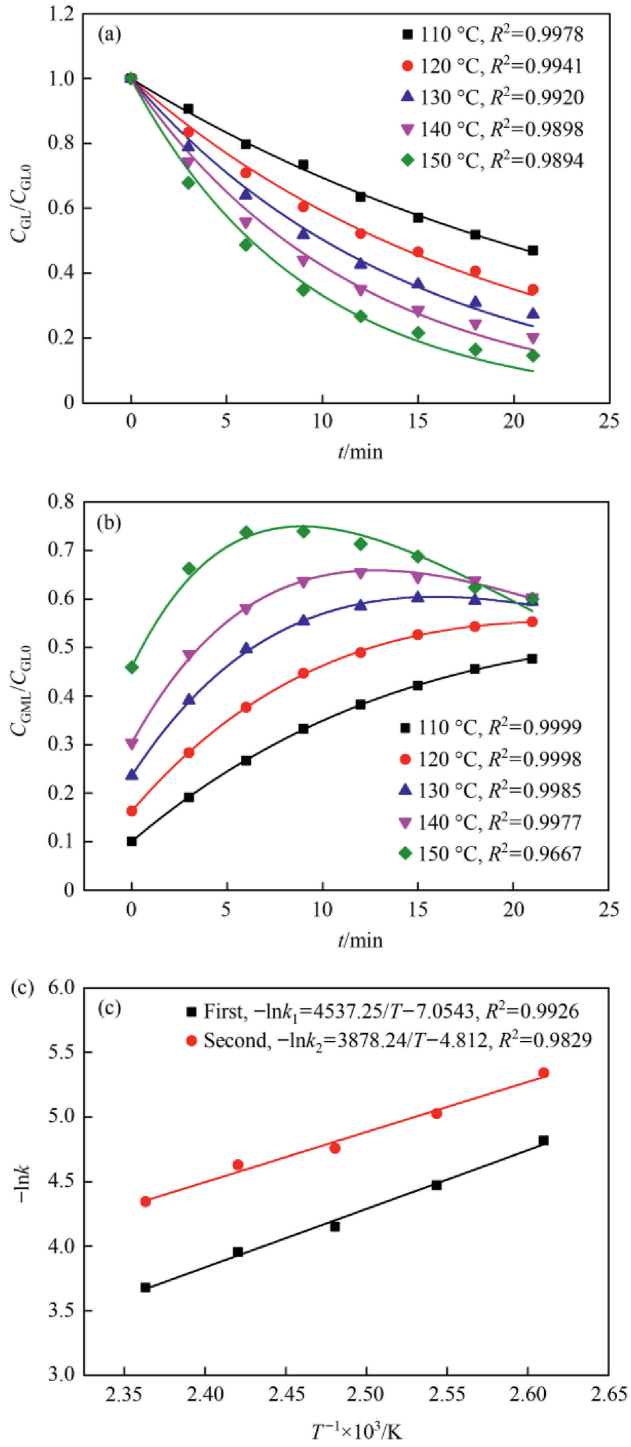

Fig. 7. Plot of (a) C_{GL}/C_{GL0} of Eq. (11), (b) C_{GML}/C_{GL0} *versus* *t* of Eq. (12) at 383.15–423.15 K and 1% *p*-toluenesulfonic acid, (c) Plot of −ln*k* *versus* 1000/*T* at 383.15–423.15 K and 1% *p*-toluenesulfonic acid.

$$k_1 = (276 + 92261X_{cat})\exp\left(\frac{-37720}{RT}\right) \quad (38)$$

$$k_2 = (80 + 4413X_{cat})\exp\left(\frac{-32240}{RT}\right) \quad (39)$$

To compare with the kinetic parameters reported in other literatures, Table 3 is as follows. In this work, the rate constants k_1 and k_2 calculated are 4.57 × 10^{-4} and 1.83 × 10^{-4} L·mol^{-1}·s^{-1} at the reaction temperature of 403 K and the molar content of catalyst of 2.0%. Compared with the other rate constants of the second-order kinetic model, the kinetic results are larger and more intrinsic. In addition, the amount of the catalyst *p*-toluenesulfonic acid was considered in the kinetic equations to make the equation more accurate.

Table 1
Values of kinetic rate constants and activation energies

T/K	k_1/L·mol^{-1}·s^{-1}	k_2/L·mol^{-1}·s^{-1}	E_1/kJ·mol^{-1}	E_2/kJ·mol^{-1}
383.15	1.35×10^{-4}	7.98×10^{-5}	37.72	32.56
393.15	1.90×10^{-4}	1.10×10^{-4}		
403.15	2.63×10^{-4}	1.43×10^{-4}		
413.15	3.20×10^{-4}	1.63×10^{-4}		
423.15	4.22×10^{-4}	2.17×10^{-4}		

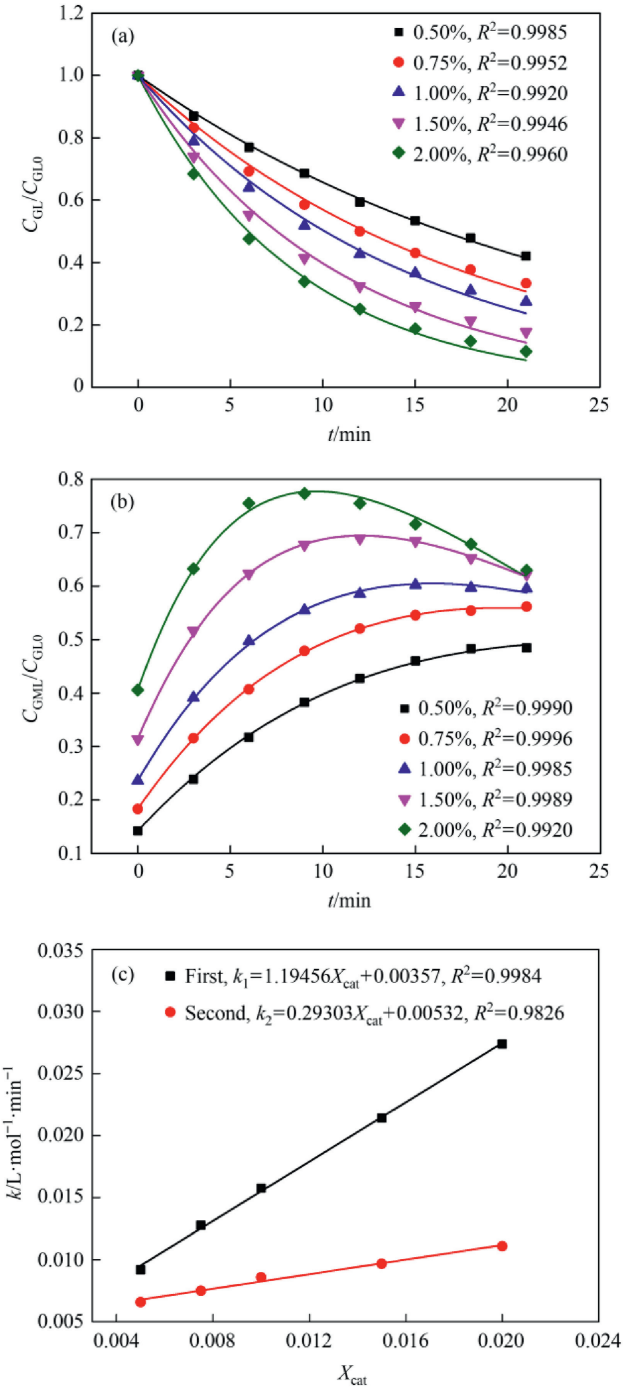

Fig. 8. Plot of (a) C_{GL}/C_{GL0}, (b) C_{GML}/C_{GL0} *versus* t at 403.15 K and 0.5%–2% *p*-toluenesulfonic acid, (c) Plot of k *versus* X_{cat} at 403.15 K and 0.5%–2% *p*-toluenesulfonic acid.

3.3. Discussion on relationship of mass transfer and kinetics results

The kinetic experimental results are obtained under homogeneous conditions, and eliminating the influence of mass transfer on the reaction. In industrial production, the esterification reaction of GL and LA is heterogeneous. It is very important to determine whether the esterification reaction is controlled by reaction kinetics or mass transfer process for industrial synthesis of GML. According to the kinetic results, the reaction rate of the main reaction and the side reaction are similar, but the main reaction has the effect of interfacial mass transfer. If the reaction rate of the main reaction is limited by mass transfer, it is beneficial to the side reaction. Therefore, the matching problem of main reaction rate and mass transfer rate is mainly discussed. The Hatta number is used to evaluate the limitation of mass transfer on reaction [29]. In general, the calculation equation of Hatta number is defined as follows [30].

$$Ha = \frac{\sqrt{\frac{2}{m+1} k_1 D_G C_G^{m-1} C_{LA}^n}}{k_L} \tag{40}$$

where, k_1 is reaction rate constant of monoesterification reaction, D_G is diffusion coefficient of GL in LA, C_G is GL concentration, C_{LA} is LA concentration, k_L is mass transfer coefficient, m and n are the reaction order of reactants GL and LA, respectively.

The previous kinetic studies have confirmed that the reaction orders for GL and LA are all 1. Therefore, Eq. (40) can be simplified to Eq. (41).

$$Ha = \frac{\sqrt{k_1 D_G C_{LA}}}{k_L} \tag{41}$$

According to literature reports, when the $Ha \geq 3$, mass transfer has a strong limitation on the reaction process, which means that the reaction is controlled by mass transfer due to the fast reaction rate; there are no mass transfer limitations when the $Ha \leq 0.3$, at this time, the reaction rate is slow and the reaction is controlled by kinetics; when the Ha between 0.3 and 3, reaction process only exists a weak mass transfer limitation [31].

The diffusion coefficient D_G can be calculated by the Wilke-Chang equation [32].

$$D_G = \frac{7.4 \times 10^{-11} (\varphi M_{LA})^{1/2} T}{\mu_{LA} V_G^{0.6}} \tag{42}$$

where, φ is association factor (estimated as 1.9 [33]), M_{LA} is LA molecular weight (200 g·mol^{-1}), T is the temperature, μ_{LA} is LA viscosity (estimated as 4 mPa·s), V_G is GL molar volume (86.9 cm^3·mol^{-1}).

The temperature and catalyst dosage of direct esterification are selected as 180 °C and 2%, respectively. D_G is estimated as 2.64×10^{-9} m^2·s^{-1} from Eq. (42), k_1 is estimated as 1.58×10^{-3} L·mol^{-1}·s^{-1} from Eq. (38), C_{LA} is estimated as 3 mol·L^{-1}. The results are displayed in Fig. 9.

Fig. 9 shows the dependence of the Hatta number on the mass transfer coefficient. When mass transfer coefficient $k_L \geq 10^{-5}$, the reaction process of LA and GL is controlled by the kinetic process. When mass transfer coefficient $k_L \leq 10^{-6}$, the reaction process is controlled by the mass transfer. The mass transfer coefficient k_L of a general reactor ranges from 10^{-7}–10^{-6} [34]. Therefore, the mass

Table 2
Values of kinetic rate constants, reaction order, and preexponential factors

X/%	k_1/L·mol^{-1}·s^{-1}	k_2/L·mol^{-1}·s^{-1}	ak_{10}/L·mol^{-1}·s^{-1}	bk_{10}/L·mol^{-1}·s^{-1}	bk_{10}/L·mol^{-1}·s^{-1}	bk_{20}/L·mol^{-1}·s^{-1}
0.50	1.53×10^{-4}	1.10×10^{-4}	276	92261	80	4413
0.75	2.13×10^{-4}	1.25×10^{-4}				
1.00	2.63×10^{-4}	1.43×10^{-4}				
1.50	3.57×10^{-4}	1.62×10^{-4}				
2.00	4.57×10^{-4}	1.83×10^{-4}				

Table 3
Comparison of the kinetic parameters

Number	Kinetic model	Reversibility	Solvent	Catalyst	Temperature/K	Reaction rate		Ref.
						k_1	k_2	
1	First-order	Irreversible	Lauric acid	Zeolite Y	403	1.22×10^{-4} s^{-1}	–	[17]
	Second-order	Irreversible				1.13×10^{-4} L·mol^{-1}·s^{-1}	–	
2	Second-order	Irreversible	Glycerol	[DMBPSH] $H_3SiW_{12}O_4$	418–433	$k_1 = 6.65 \exp\left(\frac{-39490}{RT}\right)$	–	[18]
3	Pseudo-second-order	Irreversible	Glycerol	DES [TPAB:B(OH)$_3$]	403	1.18×10^{-4} L·mol^{-1}·s^{-1}	–	[19]
					413	1.51×10^{-4} L·mol^{-1}·s^{-1}	–	
					423	1.97×10^{-4} L·mol^{-1}·s^{-1}	–	
					433	2.36×10^{-4} L·mol^{-1}·s^{-1}	–	
4	First-order	Irreversible	Lauric acid	Sodium soaps	413	3.35×10^{-5} s^{-1}	1.51×10^{-5} s^{-1}	[20]
					423	5.90×10^{-5} s^{-1}	2.67×10^{-5} s^{-1}	
					433	6.94×10^{-5} s^{-1}	3.14×10^{-5} s^{-1}	
				Potassium soaps	413	1.91×10^{-5} s^{-1}	0.95×10^{-5} s^{-1}	
					423	4.66×10^{-5} s^{-1}	2.25×10^{-5} s^{-1}	
					433	4.74×10^{-5} s^{-1}	2.26×10^{-5} s^{-1}	
5	First-order	Irreversible	Lauric acid	Zinc carboxylates	423	8.10×10^{-5} s^{-1}	4.40×10^{-5} s^{-1}	[21]
6	First-order	Irreversible	Glycerol	[DMBPSH] HSO_4/SG	403	7.33×10^{-4} s^{-1}	6.91×10^{-4} s^{-1}	[22]
					408	8.09×10^{-4} s^{-1}	7.66×10^{-4} s^{-1}	
					413	9.02×10^{-4} s^{-1}	8.54×10^{-4} s^{-1}	
					418	1.03×10^{-3} s^{-1}	9.78×10^{-4} s^{-1}	
7	Pseudo-first-order	Irreversible	Lauric acid	*p*-Toluenesulfonic acid	383–423	$k_1 = (276 + 92261X_{cat})\exp\left(\frac{-37720}{RT}\right)$	$k_2 = (80 + 4413X_{cat})\exp\left(\frac{-32240}{RT}\right)$	This work

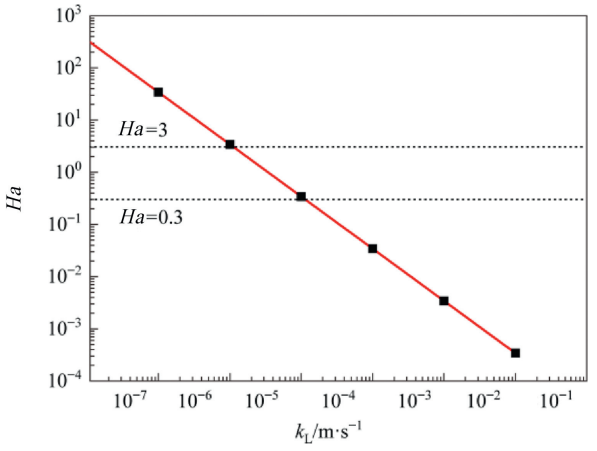

Fig. 9. Plot of *Ha versus* k_L coefficient.

transfer process cannot be ignored in the synthesis of GML with a heterogeneous system. In this work, excess LA was used to make the system homogeneous and the effect of different rotational speed on the esterification reaction was investigated by experiments. It eliminated the influence of mass transfer process on the reaction and made the kinetic results more intrinsic. Moreover, when increasing the amount of catalyst or raising temperature, the influence of mass transfer resistance will be more obvious as the kinetic constants increase. The value of k_L is closely related to the characteristic of the reactor. For direct esterification of LA with GL, it is necessary to select a suitable reactor.

4. Conclusions

In this work, the intrinsic kinetics of the consecutive reaction of GL and LA is studied. The influence of mass transfer and reversible reaction is eliminated by using the experimental condition of excessive LA, so the kinetic results are more accurate. The equilibrium reactions between isomers of GML and glycerol dilaurate (GDL) are found, which are faster than the esterification reaction. A complete kinetic model of the esterification reaction is established. According to the mathematical model of the reaction, the kinetic characteristics of the esterification reaction are experimentally studied. Experimental data is in good consistency with the mathematical model, the correlation coefficients (R^2) of each plot are basically above 0.99. Therefore, the measurement method of intrinsic kinetics of esterification reaction and mathematical model can be used for the measurement of kinetics of other consecutive esterification reactions. The catalytic process of *p*-toluenesulfonic acid is discussed and demonstrated experimentally. The kinetic equations of the consecutive esterification reaction were obtained as $k_1 = (276 + 92261X_{cat})\exp(-37720/RT)$ and $k_2 = (80 + 4413X_{cat})\exp(-32240/RT)$. The kinetic results are beneficial to the optimization of operating conditions and reactor design in GML production process. In addition, the amount of the catalyst *p*-toluenesulfonic acid was considered in the kinetic equations to make the equation more accurate and make it suitable for various situations with different catalyst amounts in industrial production.

Based on the kinetic results, the influence of mass transfer process on the reaction is discussed. When mass transfer coefficient $k_L \geq 10^{-5}$, the reaction process of LA and GL is controlled by the kinetic process. When mass transfer coefficient $k_L \leq 10^{-6}$, the reaction process is controlled by the mass transfer. Under the condition of high temperature and large amounts of catalyst, the influence of mass transfer process should be considered even more. A suitable reactor should be selected to intensify the reaction process. The results of kinetic study also show that the reaction rate constants of consecutive esterification are all in the same order of magnitude. In order to improve the selectivity of monoesters, the future research direction should focus on the development of selective catalysts.

Declaration of Interest

The authors declare that they have no known competing financial interests or personal relationships that could have appeared to influence the work reported in this article.

CRediT Authorship Contribution Statement

Han-Qiao Hu: Writing – original draft. Yue Zhang: Writing – review & editing. Ming Fan: Conceptualization. Yong Cai: Conceptualization. Guang-Wen Chu: Resources. Liang-Liang Zhang: Conceptualization, Resources.

Acknowledgements

This work was financially supported by the National Research and Development Program of China (2021YFC3001100) and the National Natural Science Foundation of China (22288102).

Nomenclature

C_j	j concentration, $mol \cdot L^{-1}$
D_G	diffusion coefficient of glycerol in lauric acid, $m^2 \cdot s^{-1}$
E	activation energy of reaction, $J \cdot mol^{-1}$
Ha	Hatta number
k	overall reaction rate constant, $L \cdot mol^{-1} \cdot s^{-1}$
k_j	reaction kinetic rate constant in dynamics, $L \cdot mol^{-1} \cdot s^{-1}$
k_L	mass transfer coefficient, $m \cdot s^{-1}$
k_0	pre-exponential factor, $L \cdot mol^{-1} \cdot min^{-1}$
M_{LA}	lauric acid molecular weight, $g \cdot mol^{-1}$
m	reaction order of glycerol
n	reaction order of lauric acid
R	gas constant, 8.314 $J \cdot mol^{-1} \cdot K^{-1}$
T	temperature, K
t	reaction time, s
V_G	glycerol molar volume, $cm^3 \cdot mol^{-1}$
X_{cat}	molar content of catalyst in glycerol
μ_{LA}	lauric acid viscosity, $mPa \cdot s$
φ	association factor

References

[1] P.M. Schlievert, S.H. Kilgore, K.S. Seo, D.Y.M. Leung, Glycerol monolaurate contributes to the antimicrobial and anti-inflammatory activity of human milk, *Sci. Rep.* 9 (1) (2019) 14550.
[2] F. Chen, G. Zhang, C. Liu, J. Zhang, F. Zhao, B. Xu, Highly selective synthesis of monolaurin via enzymatic transesterification under batch and continuous flow conditions, *J. Oleo Sci.* 68 (11) (2019) 1125–1132.
[3] P.M. Schlievert, M.L. Peterson, Glycerol monolaurate antibacterial activity in broth and biofilm cultures, *PLoS One* 7 (7) (2012) e40350.
[4] X.J. Chen, D. Wu, Y. He, S. Liu, Detecting the quality of glycerol monolaurate: a method for using Fourier transform infrared spectroscopy with wavelet transform and modified uninformative variable elimination, *Anal. Chim. Acta* 638 (1) (2009) 16–22.
[5] M.S. Zhang, A. Sandouk, J.C.D. Houtman, Glycerol monolaurate (GML) inhibits human T cell signaling and function by disrupting lipid dynamics, *Sci. Rep.* 6 (2016) 30225.
[6] P. Lozano, C. Gomez, S. Nieto, G. Sanchez-Gomez, E. García-Verdugo, S.V. Luis, Highly selective biocatalytic synthesis of monoacylglycerides in sponge-like ionic liquids, *Green Chem.* 19 (2) (2017) 390–396.
[7] L. Hermida, A.Z. Abdullah, A.R. Mohamed, Synthesis of monoglyceride through glycerol esterification with lauric acid over propyl sulfonic acid post-synthesis functionalized SBA-15 mesoporous catalyst, *Chem. Eng. J.* 174 (2–3) (2011) 668–676.
[8] F. Hamerski, M.L. Corazza, LDH-catalyzed esterification of lauric acid with glycerol in solvent-free system, *Appl. Catal. Gen.* 475 (2014) 242–248.
[9] S. Baum, E. Ritter, I. Smirnova, M. Schilling, A. Liese, The role of phase behavior in the enzyme catalyzed synthesis of glycerol monolaurate, *RSC Adv.* 6 (38) (2016) 32422–32429.
[10] N. Siri-nguan, C. Ngamcharussrivichai, Alkoxide-intercalated Mg–Al layered double hydroxides as selective catalysts forthe synthesis of monoglycerides, *React. Kinet. Mech. Catal.* 119 (1) (2016) 273–289.
[11] W.B. Setianto, T.Y. Wibowo, H. Yohanes, F. Illaningtyas, D.D. Anggoro, Synthesis of glycerol mono-laurate from lauric acid and glycerol for food antibacterial additive, *IOP Conf. Ser. Earth Environ. Sci.* 65 (2017) 012046.
[12] R. Chakraborty, E. Mandal, Fast and energy efficient glycerol esterification with lauric acid by near and far-infrared irradiation: taguchi optimization and kinetics evaluation, *J. Taiwan Inst. Chem. Eng.* 50 (2015) 93–99.
[13] S.S. Miao, X. Li, Enzymatic esterification of lauric acid to give monolaurin in a microreactor, *J. Chem. Res.* 45 (7–8) (2021) 660–667.
[14] Y.N. Sun, J.L. Hu, S. An, Q.Q. Zhang, Y.H. Guo, D.Y. Song, Q.K. Shang, Selective esterification of glycerol with acetic acid or lauric acid over rod-like carbon-based sulfonic acid functionalized ionic liquids, *Fuel* 207 (2017) 136–145.
[15] N. Arpi Satriana, Y.M. Lubis, Adisalamun, M.D. Supardan, W.A.W. Mustapha, Diacylglycerol-enriched oil production using chemical glycerolysis, *Eur. J. Lipid Sci. Technol.* 118 (12) (2016) 1880–1890.
[16] D.M. Lai, L. Deng, J. Li, B. Liao, Q.X. Guo, Y. Fu, Hydrolysis of cellulose into glucose by magnetic solid acid, *ChemSusChem* 4 (1) (2011) 55–58.
[17] H. Oktavianty, S.B. Sasongko, L. Buchori, D.D. Anggoro, Kinetic study of glycerol monolaurate (GML) production from glycerol with lauric acid using a dealuminated zeolite Y catalyst, *IOP Conf. Ser. Mater. Sci. Eng.* 1053 (1) (2021) 012060.
[18] X.X. Han, X.F. Zhang, G.Q. Zhu, J.J. Liang, X.H. Cao, R.J. Kan, C.T. Hung, L.L. Liu, S. B. Liu, Ionic liquid–silicotungstic acid composites as efficient and recyclable catalysts for the selective esterification of glycerol with lauric acid to monolaurin, *ChemCatChem* 9 (14) (2017) 2727–2738.
[19] Z.L. Shen, L.F. Chen, H.Y. Cheng, Z.W. Qi, Selective synthesis of glyceryl monolaurate intensified by boric acid based deep eutectic solvent, *Catal. Today* 407 (2023) 291–300.
[20] H. Szela›g, W. Zwierzykowski, Esterification kinetics of glycerol with fatty acids in the presence of sodium and potassium soaps, *Lipid Fett* 100 (7) (1998) 302–307.
[21] A. Macierzanka, H. Szelag, Esterification kinetics of glycerol with fatty acids in the presence of zinc carboxylates: preparation of modified acylglycerol emulsifiers, *Ind. Eng. Chem. Res.* 43 (24) (2004) 7744–7753.
[22] X.X. Han, G.Q. Zhu, Y.X. Ding, Y.L. Miao, K.W. Wang, H.J. Zhang, Y.B. Wang, S.B. Liu, Selective catalytic synthesis of glycerol monolaurate over silica gel-based sulfonic acid functionalized ionic liquid catalysts, *Chem. Eng. J.* 359 (2019) 733–745.
[23] P.Y. Hoo, A.Z. Abdullah, Direct synthesis of mesoporous 12-tungstophosphoric acid SBA-15 catalyst for selective esterification of glycerol and lauric acid to monolaurate, *Chem. Eng. J.* 250 (2014) 274–287.
[24] Y. Li, Y. Zou, H. Xu, R.N. He, Y. Muhammad, Z.F. Tong, Preparation of *n*-amyl acetate *via* esterification of acetic acid and *n*-amyl alcohol using[HSO_3pmim][HSO_4]/SiO_2 as catalyst: catalyst preparation, characterization and reaction kinetics, *Chem. Eng. J.* 410 (2021) 128282.
[25] S. Jiang, Z.X. Zeng, W.L. Xue, W. Zhang, Z.Y. Zhou, Kinetic study on the reaction of palmitic acid with ethanol catalyzed by deep eutectic solvent based on dodecyl trimethyl ammonium chloride, *Korean J. Chem. Eng.* 37 (9) (2020) 1482–1489.
[26] M. Berrios, J. Siles, M. Martin, A. Martin, A kinetic study of the esterification of free fatty acids (FFA) in sunflower oil, *Fuel* 86 (15) (2007) 2383–2388.
[27] R. Nakamura, K. Komura, Y. Sugi, The esterification of glycerine with lauric acid catalyzed by multi-valent metal salts. Selective formation of mono- and dilaurins, *Catal. Commun.* 9 (4) (2008) 511–515.
[28] K. Mamtani, K. Shahbaz, M.M. Farid, Glycerolysis of free fatty acids: a review, *Renew. Sustain. Energy Rev.* 137 (2021) 110501.
[29] Y.Y. Zhan, J. Shi, M.J. Su, Y. Luo, G.W. Chu, H.K. Zou, J.F. Chen, Kinetics of catalytic oxidation of sodium ethyl mercaptide, *Chem. Eng. Sci.* 217 (2020) 115516.
[30] H.P.L. Gemoets, Y.H. Su, M.J. Shang, V. Hessel, R. Luque, T. Noël, Liquid phase oxidation chemistry in continuous-flow microreactors, *Chem. Soc. Rev.* 45 (1) (2016) 83–117.

[31] J. Fischer, T. Lange, R. Boehling, A. Rehfinger, E. Klemm, Uncatalyzed selective oxidation of liquid cyclohexane with air in a microcapillary reactor, *Chem. Eng. Sci.* 65 (16) (2010) 4866–4872.
[32] Z.K. Yazdi, I. Alemzadeh, Kinetic mechanism of conjugated linoleic acid esterification and production of enriched glycerides as functional oil, *Can. J. Chem. Eng.* 95 (11) (2017) 2078–2086.
[33] G. Gofferjé, A. Stäbler, T. Herfellner, U. Schweiggert-Weisz, E. Flöter, Kinetics of enzymatic esterification of glycerol and free fatty acids in crude Jatropha oil by immobilized lipase from *Rhizomucor Miehei*, *J. Mol. Catal. B Enzym.* 107 (2014) 1–7.
[34] Y.D. Zhang, L.L. Zhang, Z.X. Wang, B.C. Sun, G.W. Chu, J.F. Chen, Liquid-liquid heterogeneous mixing efficiency in a rotating packed bed reactor, *AIChE. J.* 69 (6) (2023) e18000.